

Semi-Meissner state and non-pairwise intervortex interactions in type-1.5 superconductors

Johan Carlstrom^{1,2}, Julien Garaud^{2,1}, Egor Babaev^{2,1}

¹ Department of Theoretical Physics The Royal Institute of Technology Stockholm SE-10691 Sweden

² Department of Physics University of Massachusetts Amherst MA 01003 USA

We demonstrate existence of *non-pairwise* interaction forces between vortices in multicomponent and layered superconducting systems. That is, in contrast to most common models, the interactions in a group of such vortices is not a universal superposition of Coulomb or Yukawa forces. Next we consider the properties of vortex clusters in Semi-Meissner state of type-1.5 two-component superconductors. We show that under certain condition non-pairwise forces can contribute to formation of very complex vortex states in type-1.5 regimes.

I. INTRODUCTION

The crucial importance of topological excitations in the physics of superconductivity made quantum vortex solutions in the Ginzburg-Landau (GL) models perhaps the most studied examples of topological solitons (defined as localized lumps of energy characterized by a topological invariant)^{1,2}. These well studied vortex solutions are frequently used as generic testing objects for High Energy Physics and Cosmological models¹. In that broader context, especially spectacular theoretical works attempted on numerous occasions to identify topological solitons in the Skyrme and Faddeev models with particles¹. There the particle-solitons are lumps of energy which enjoy a topological protection against radiating their energy. Superconducting vortices, in spite being known to form a variety of “aggregate” vortex states: vortex liquids, glasses etc still do not show nearly as complex ground states as e.g. the Skyrme or Faddeev models¹ because of the smaller diversity of known intervortex interaction potentials. The recent works on multicomponent superconductors aimed at realizing more complex bound multi-vortex states in the so-called “type-1.5 regime”. In that regime, due to existence of two components, thermodynamically stable vortex solutions were found that exhibit strongly non-monotonic interaction potentials between two vortices, with short-range repulsive and long-range attractive parts³ and thus form vortex clusters in low magnetic fields. After the recent experimental publications⁴ this physics received increased attention (see e.g.⁶).

In this work we investigate the structure of multi-vortex bound states in two-component superconductors beyond the validity of the linearized theory and find *non-pairwise multi-body interactions* which are especially pronounced at short intervortex separations. We show that in certain cases the non-pairwise forces are strong enough to lead to extremely rich multivortex states. We also propose how these vortex states can be experimentally realized in layered superconducting structures.

We consider a Ginzburg-Landau model of a two-component superconductor which appears in various physical systems ranging from multiband and layered superconductors to projected states of metallic hydrogen and models of neutron stars

interior⁵.

$$\mathcal{F} = \frac{1}{2} \sum_{i=1,2} \left[|(\nabla + ie\mathbf{A})\psi_i|^2 + (2\alpha_i + \beta_i|\psi_i|^2)|\psi_i|^2 \right] + \frac{1}{2} (\nabla \times \mathbf{A})^2 - \eta |\psi_1| |\psi_2| \cos(\theta_2 - \theta_1) \quad (1)$$

Here e is the electric charge, $\psi_{1,2} = |\psi_{1,2}|e^{i\theta_{1,2}}$ represent the superconducting components coupled by the gauge field \mathbf{A} and the Josephson coupling η . For a microscopic derivation of such model for two-band superconductors see⁷. It was demonstrated recently in the framework of a self-consistent microscopic theory that this “minimalistic” two-band model describes qualitatively well intervortex interaction in multiband superconductor in a rather wide range of temperatures⁸. We choose the units where $\hbar = c = 1$.

The key feature of the model is that one-flux quantum vortices induced by magnetic field are “composite”. That is, they have a core around which both phases wind by 2π , i.e. $\Delta\theta_{1,2} = \oint_C \nabla\theta_{1,2} d\ell = 2\pi$ (C being a closed path around the vortex core). One-quanta vortex can thus be viewed here as a bound state of two “fractional” vortices^{9–11}. The model exhibits type-1.5 superconductivity when the magnetic field penetration length scale λ is smaller than one of the characteristic length scales of the density variation $\xi_{1,2}$ and also the conditions for short range repulsion and thermodynamical stability are satisfied³. In the type-1.5 regime two vortices with similar circulation have interaction that is attractive at long range (driven by density-density interaction) but repulsive at short range (due to current-current and magnetic interaction)³. This results in a formation of a “semi-Meissner” state in low magnetic fields where vortex clusters coexist with two-component Meissner state. The magnetization curves of a type-1.5 superconductor are schematically shown on Fig. 1.

We consider below two types of systems: (i) two-band and layered superconducting systems with weak and strong Josephson coupling and (ii) the systems where there is no Josephson coupling. The latter situation occurs in the context of the theories of liquid metallic hydrogen, deuterium and their mixtures^{10,11}, and physics of neutron star interiors, where the two fields represent electronic, protonic and Σ^- hyperon Cooper pair condensates¹² (for literature overview see⁵). Because one cannot convert, say, electrons to protons or deuterons, the intercomponent Josephson coupling in this case is forbidden on symmetry grounds but the condensates are coupled by the vector potential. Experimentally the type-1.5-like physics can be also realized in a system of interlaced

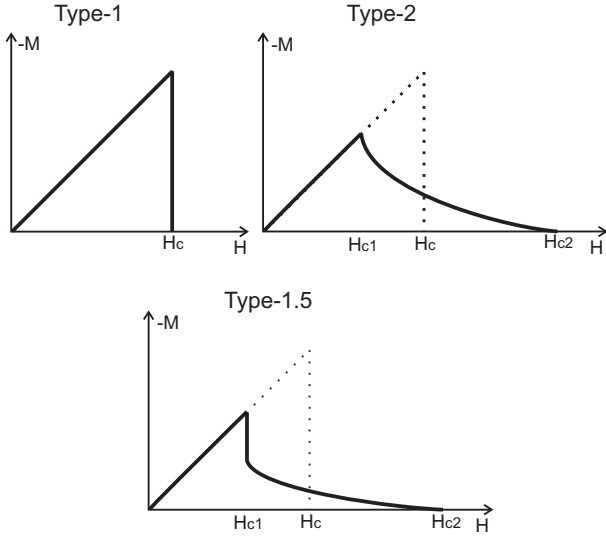


Figure 1. A schematic picture of magnetization curves of type-I, type-II and type-1.5 superconductors. Type-1.5 superconductor has a first order phase transition in low magnetic fields. In low magnetic field it can support a phase separation into vortex droplets and Meissner domains (the semi-Meissner state).

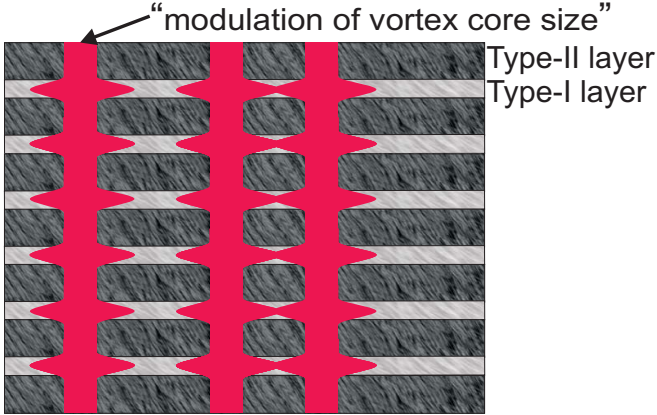


Figure 2. A schematic picture of a collection of Josephson-coupled layers of type-I and type-II superconductors. Vortices induced by magnetic field are kept in stacks by interlayer Josephson and electromagnetic coupling. If in the type-I layers the cores will extend beyond the average magnetic field penetration length, these extended cores should cause attractive interaction between these vortex lines. The system can be used to model the type-1.5 behavior.

Josephson-coupled type-I/type-II multilayers shown schematically in Fig. 2.

The usual framework within which vortex matter in superconductors and superfluids is usually discussed relies on the assumption that interactions in a system of vortices is a superposition of pairwise forces. Indeed the most usual analysis of interaction between well separated topological solitons involves linearization. By nature of this approximation, the interaction in a system of multiple vortices is a superposition of two-body forces. Similarly, for example the description of phase transitions in type-II superconductors in terms of vor-

tex loop proliferation is based on London approximation¹³. In this approximation the fluctuations of densities are neglected and the intervortex interaction is then pairwise. Non-linear effects which lead to nonpairwise contributions in the intervortex interaction are, in general, less discussed. For certain vortex configurations in a single-component Ginzburg-Landau model, nonlinear effects were studied recently in¹⁴.

Here we demonstrate the importance of complicated non-pairwise forces between superconducting vortices arising in multicomponent systems. It has particularly important consequences for vortex clusters in the type-1.5 regime (though also relevant for type-II two band superconductors).

II. THREE-BODY INTERVORTEX FORCES

First, let us present a highly accurate numerical study of a three body vortex problem. The interaction between vortices was investigated as follows (for a detailed description see appendix A): First a vortex pair is fixed in the center of the system. A third vortex is then inserted, and the energy is minimized with respect to all the degrees of freedom, except the positions of the centers of the vortex cores in the first component. The procedure is then repeated for different positions of the third vortex. The resulting interaction energy is shown on Fig. 3 which shows pronounced violation of the superposition principle for intervortex forces in this system. To minimize the effects of discretization the calculation was performed on a ultra-high resolution grid of up to $\propto 10^7$ points, with lattice spacing $h \sim \xi_1/100$ (where ξ_1 is the coherence length of the dominant component in the limit of no coupling to the second component). We used 4-16 h on a 8-core cluster node to relax each data point in the interaction potential. We choose a “minimally invasive” procedure of pinning a vortex on a numerical grid, which gives most accurate long- and medium- range forces but, on the other hand, does not work for the (irrelevant for this study) very short intervortex distances (for details see Appendix A). Consequently in Fig. 3 no data is given for too closely placed vortices.

In all the type-1.5 regimes which we considered we found diverse and pronounced to various degrees non-pairwise interactions.

III. VORTEX CLUSTERS IN A SEMI-MEISSNER STATE AND NON-PAIRWISE INTERACTIONS.

Let us now investigate how the presence of non-pairwise interactions along with non-monotonic two-body forces affects the magnetic response. Below we report highly accurate numerical solutions for N-vortex bound states in several regimes (for technical details see Appendix B). Animations showing the evolution of the system, during the numerical energy minimization, from the various initial configurations to the vortex clusters are also available as supplementary material¹⁵.

The figures (Fig. 4–Fig. 11) show various bound states of multiple flux quanta in $U(1) \times U(1)$ as well as in Josephson-coupled $U(1)$ models. Consider first the case where $\alpha_{1,2} < 0$.

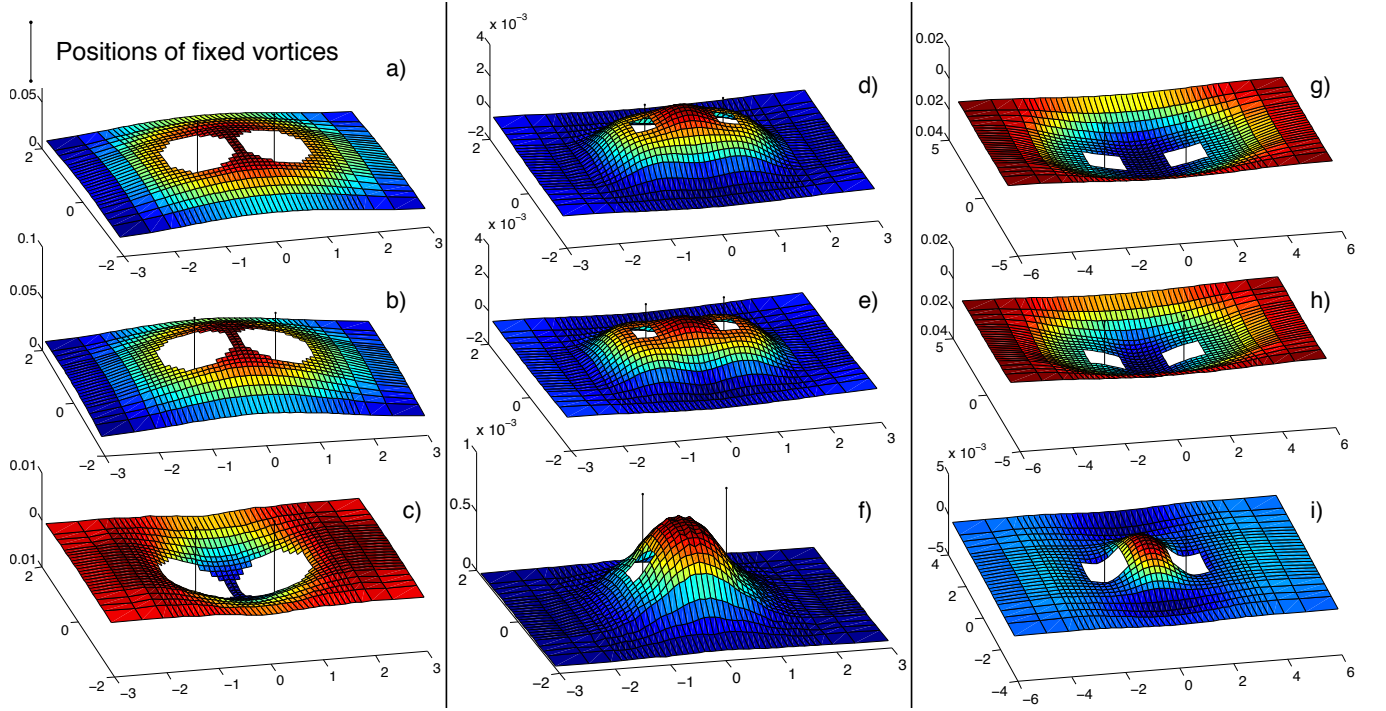


Figure 3. Interaction energy between a single vortex and a fixed vortex pair (position of the fixed vortices are shown by two black lines). GL parameters are : $(\alpha_1, \beta_1) = (-1.0, 1.0)$ and $e = 1.3$; $(\alpha_2, \beta_2) = (3.0, 0.5)$, $\eta = 3$ for panels a, b, c; $(\alpha_2, \beta_2) = (3.0, 0.5)$, $\eta = 7$ for d, e, f panels and $(\alpha_2, \beta_2) = (-0.0625, 0.25)$, $\eta = 0.5$ for panels g, h, i. Top row (a, d, g) gives the total interaction energy, while second one (b, e, h) gives the sum of pairwise interactions. The third row (c, f, i) displays the difference between these energies, which demonstrates the existence of strong nontrivial, non-pairwise, (three body) interactions. The regimes shown in the left, middle and right columns are type-II, type-I.5 and type-I correspondingly.

There appear very interesting geometrical properties of the vortex ground states (shown on Fig. 4, Fig. 5). One can clearly see that with growing number of vortices, the local vortex structure strongly depends on the number of vortices in a cluster. The striking feature which is to various degrees is manifest on all the figures is the coexistence and competition between type-II-like behavior of the first condensates which attempts to form a regular vortex lattice and type-I-like behavior of the second condensate. Namely the second condensate mimics the formation of a single large normal domain. Also like in a genuine type-I superconductor, this component has supercurrent density which is predominantly concentrated on the boundary of the domain. Clearly it energetically prefers a formation of a circular boundary. These competing tendencies in the type-I.5 system result in neither hexagonal nor circular boundary. The next visually striking effect is that the vortex solutions are very different inside the vortex cluster and on the cluster boundary. This shows up especially clearly in the current density.

The multibody forces in this nonlinear theory, originate in nontrivial deformation of vortices by their neighbors in a vortex cluster. First the qualitatively new physics which arises in these clusters is the appearance of gradients of the phase difference $\nabla(\theta_1 - \theta_2)$ between the condensate fields. It is clearly seen on the panels f from the plotted quantity $\text{Im}(\psi_1^* \psi_2)$. One of the mechanisms of the generation of the phase difference which we observed was associated with splitting of the vortex

cores of the components $\psi_{1,2}$ driven by competing interactions. It leads to a “dipole”-like configuration of the phase difference of the two components which in turn results in contributions to multi-body forces associated with the induced phase difference gradients. This splitting exists in cases of zero, as well as finite Josephson coupling, though it is smaller in the later case. We observed also more complicated configurations like “quadrupoles” of the phase difference fields. These configurations occurred when the vortices broke their axial symmetry by relegating more phase gradients in the areas where density was depleted by neighboring vortices. Another source of multibody forces was associated with nontrivial condensate densities modulations for a group of several vortices.

Note that the presence of gradients in the phase difference, along with gradients of the relative density of two condensates is known to lead to contributions from self-generated Skyrme-like terms to magnetic energy density¹⁶. This makes the physics of the two-component vortex cluster boundary and the resulting multibody forces, in general, a complicated nonlinear problem.

With increased number of vortices the simulations frequently produced long-living bound states of irregular shapes like that shown on Figs. 10 and 11.

Parameter sets where the system is close to type-I regime (like the one shown of Fig. (7)) show that the transition (in the parameter space of the model) to type-I regime manifests itself in a depletion of current densities inside vortex clusters and

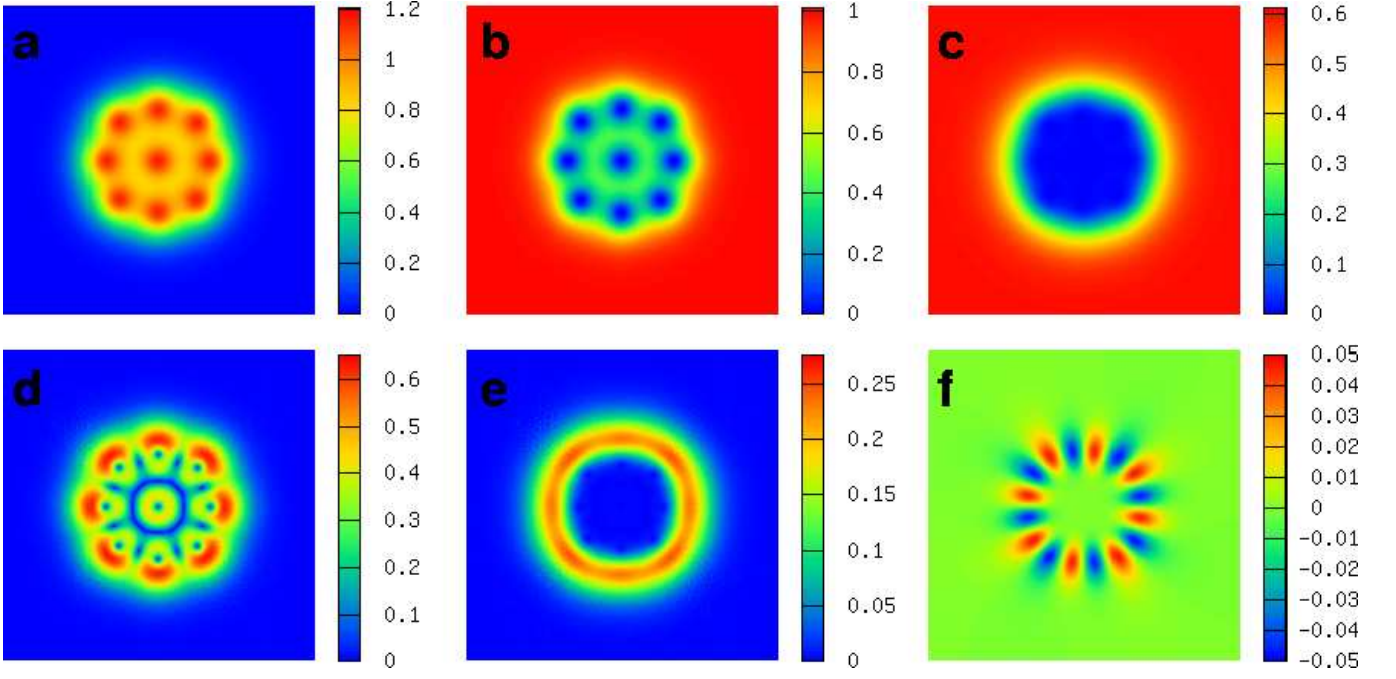


Figure 4. The ground state of a $N_v = 9$ flux quanta configuration in type-1.5 $U(1) \times U(1)$ superconductor (i.e. $\eta = 0$). The parameters of the potential are $(\alpha_1, \beta_1) = (-1.00, 1.00)$ and $(\alpha_2, \beta_2) = (-0.60, 1.00)$, while the electric charge is $e = 1.48$. The physical quantities displayed here are **a** the magnetic flux density, **b** (*resp.* **c**) is the density of the first (*resp.* second) condensate $|\psi_{1,2}|^2$. **d** (*resp.* **e**) shows the norm of the supercurrent in the first (*resp.* second) component. The panel **f** is $\text{Im}(\psi_1^* \psi_2)$ which is nonzero when there appears a difference between the phases of ψ_1^* and ψ_2 . The second component has a type-I like behavior: its density is depleted in the vortex cluster and its current is mostly concentrated on the boundary of the cluster.

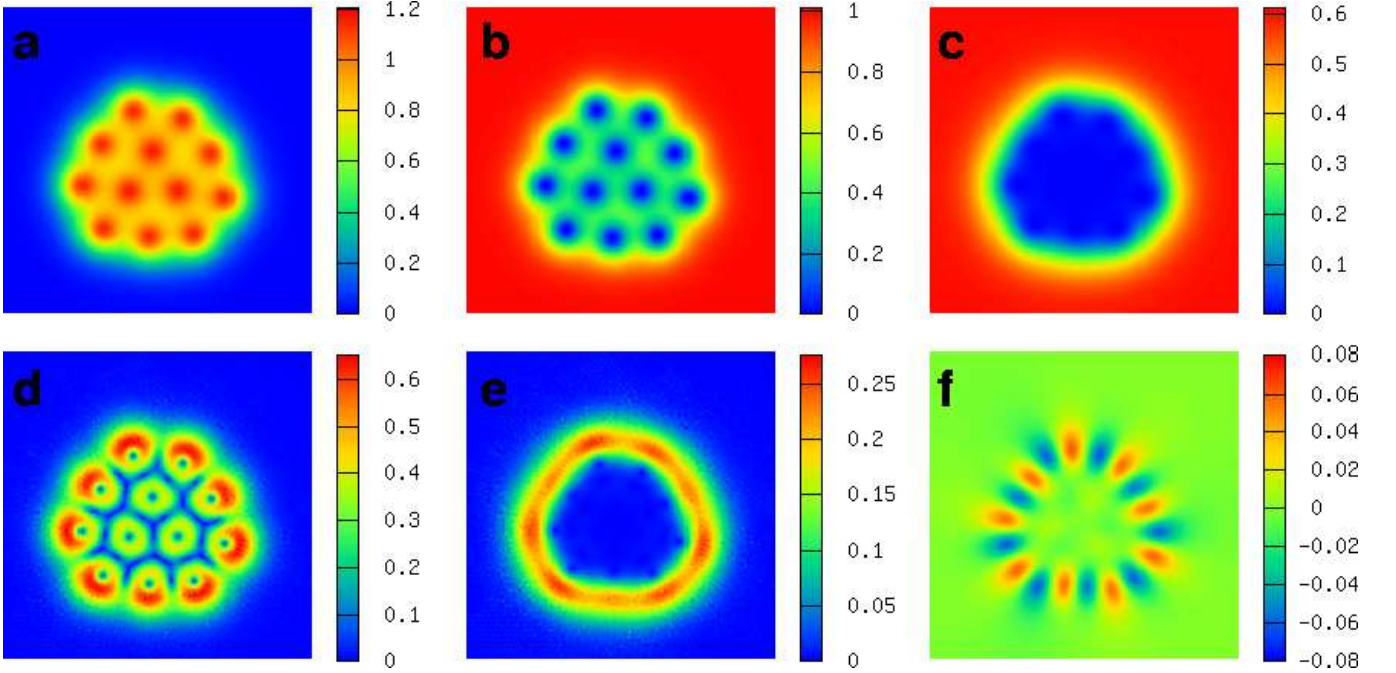


Figure 5. The ground state of a $N_v = 12$ flux quanta configuration. The parameter set is the same as in Fig. 4. Here the global 8-folded discrete symmetry of the cluster has been broken down to the 3-folded symmetry. There is a competition between type-I-like (normal circular cluster with a boundary current) and type-II-like tendencies (vortex lattice).

relative increase of current density on the cluster's boundary. In type-I regime the system forms one circular cluster where

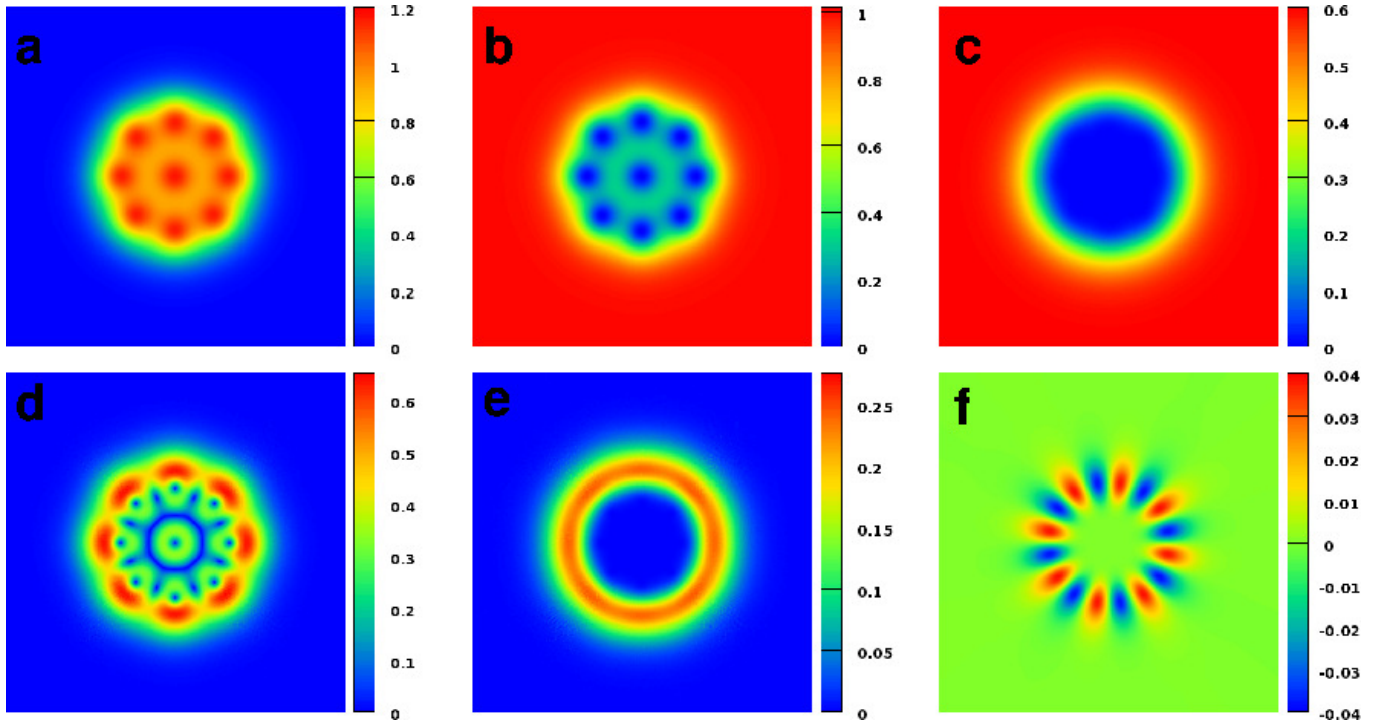


Figure 6. Ground state of 9 vortices in a $U(1) \times U(1)$ superconductor with two active bands $(\alpha_2, \beta_2) = (-0.6, 1)$ (without interband coupling). The parameter set here is as in Fig. 4 except $e = 1.55$ which places the system closer to the transition with the type-I regime. This is manifest in the more circular boundary of the cluster compared to Fig. 4.

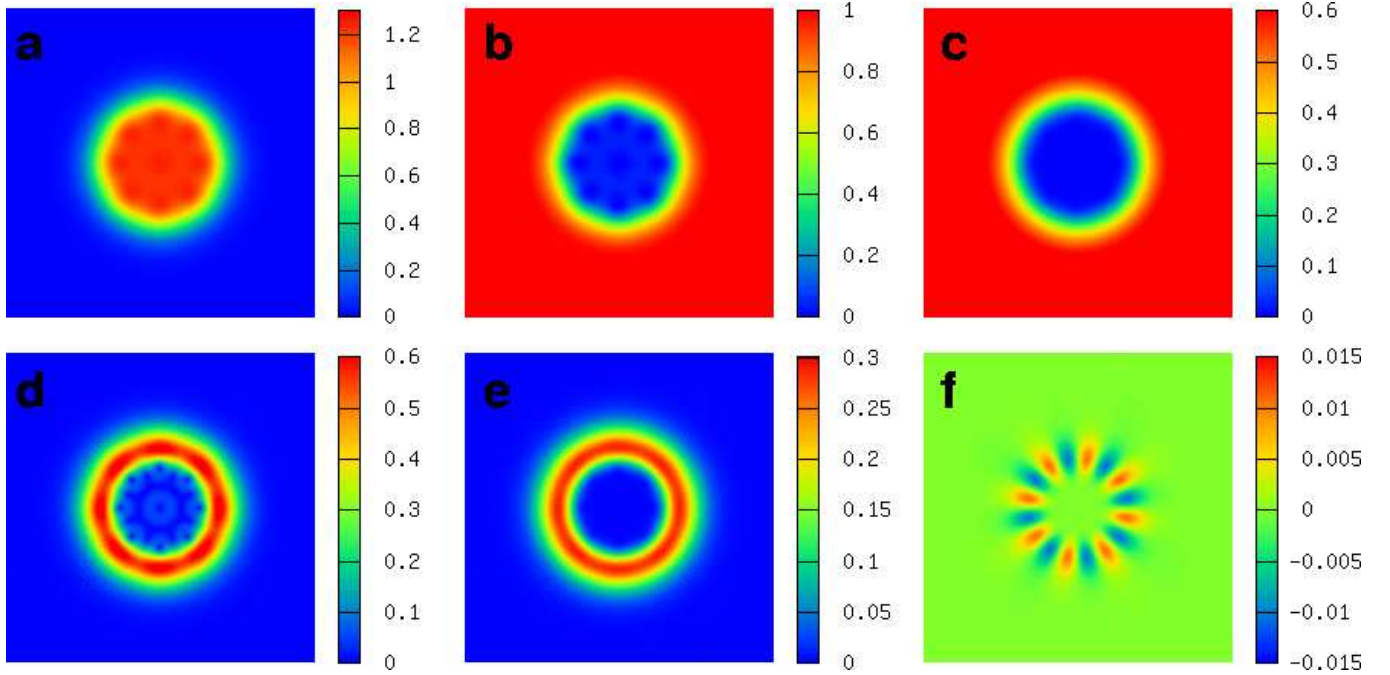


Figure 7. Ground state of an $N_v = 9$ vortex configuration with the parameter set given by Fig. 4, but with $e = 1.59$ and added Josephson coupling $\eta = 0.1$. Although the Josephson term introduced an energy penalty for phase difference, it has little effect on the vortex cluster boundary. At the boundary the competing magnetic and density-density interactions win over phase-locking terms and generates phase difference gradients. Also in this case the system is close to type-I regime: i.e. most of the current is concentrated on the boundary of the cluster.

the current is concentrated on the boundary (i.e. a single giant vortex).

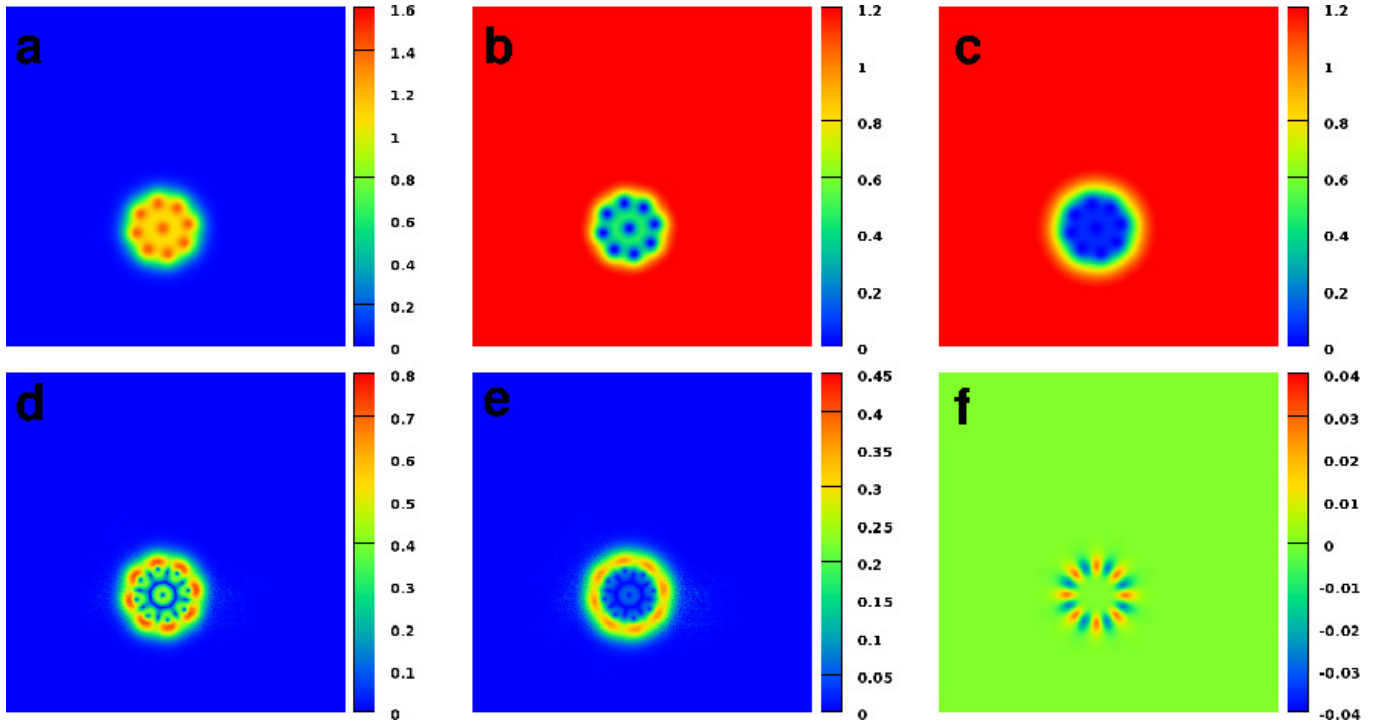


Figure 8. Ground state of 9 vortices in a superconductor with two active bands. Parameters of the interacting potential are $(\alpha_1, \beta_1) = (-1.00, 1.00)$, $(\alpha_2, \beta_2) = (-0.0625, 0.25)$ while the interband coupling is $\eta = 0.5$ which is substantially larger than on Fig. 7. The electric charge, parameterizing the penetration depth of the magnetic field, is $e = 1.30$ so that the well in the nonmonotonic interacting potential is very small. In this case there is visible admixture of the current in second component in vortices inside the cluster.

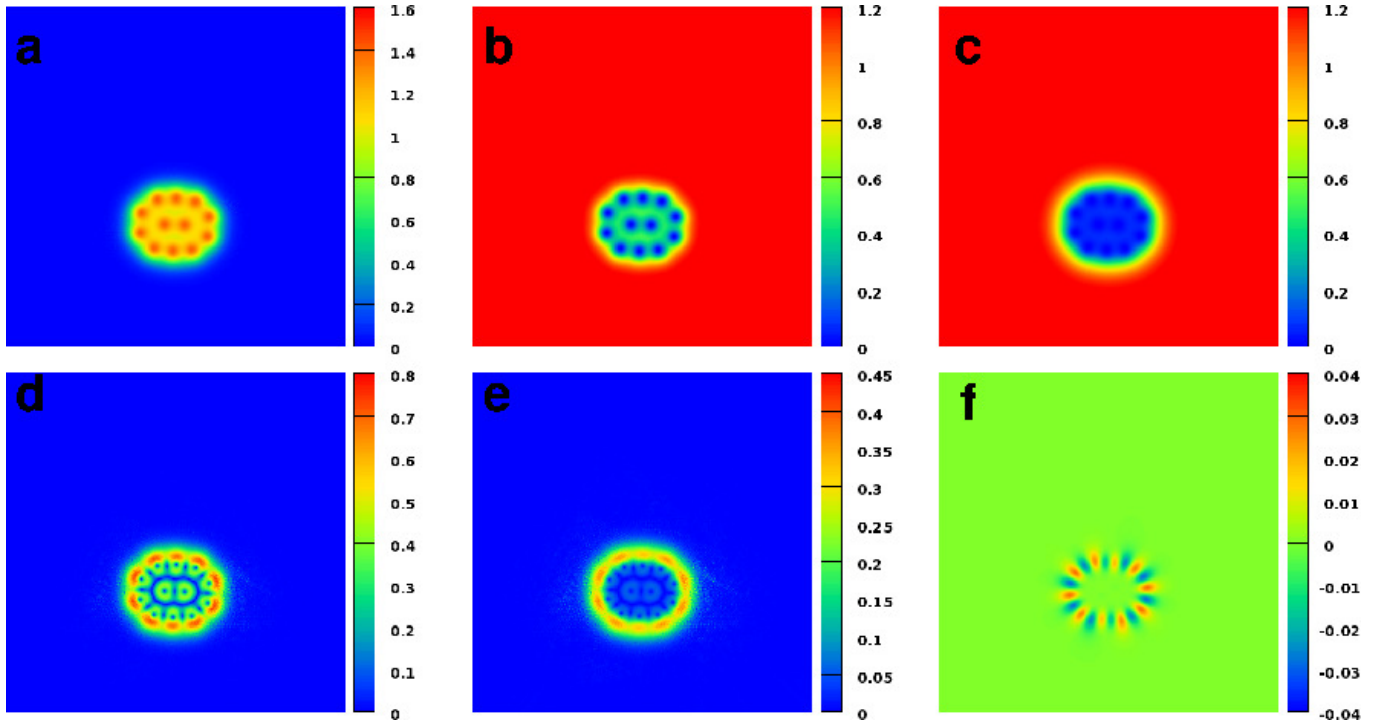


Figure 9. Ground state of $N_v = 12$ vortices, for a superconductor with broken $U(1) \times U(1)$ symmetry, with the parameters as in Fig. 8. The system compromises between both type-I-like and type-II-like tendencies in the different superconducting components.

Note that in single-component type-I superconductors the domains of normal phase have a circular boundary only when

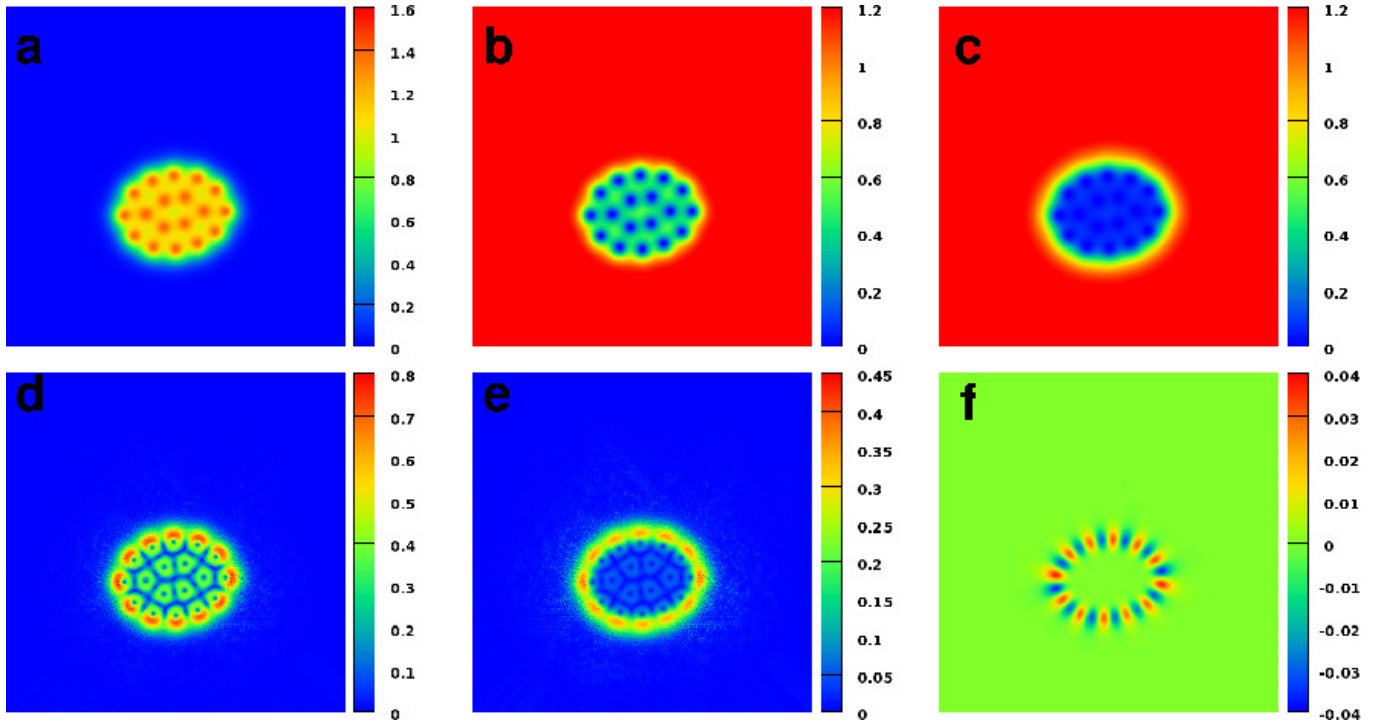


Figure 10. Elongated cluster of vortices in the same superconductor as in Fig. 8, but with $N_v = 18$ vortices.

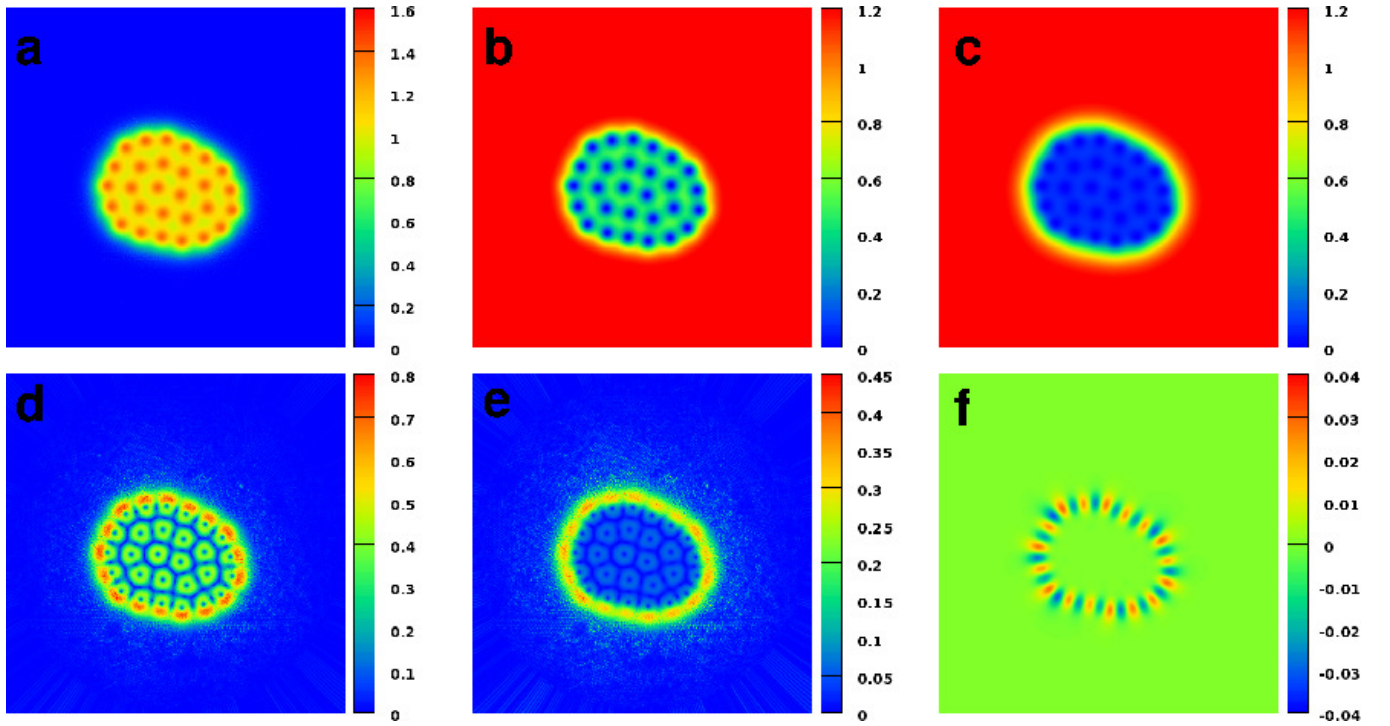


Figure 11. Bound state of $N_v = 28$ vortices, for a superconductor with broken $U(1) \times U(1)$ symmetry, with the parameters as in Fig. 8. This irregularly shaped cluster represents a local minimum of the free energy. The local minima originate from the competing interactions yielding a complicated free energy landscape.

the effects of stray fields outside sample are neglected. In finite samples of type-I superconductors the stray magnetic

fields typically lead to formation of macroscopically large stripes of the normal phase rather than circular domains²,

though other geometries were also observed¹⁷. Similarly in realistic experimental setups especially for type-1.5 bilayers, stray magnetic fields could lead to vortex stripes rather than circular vortex clusters formation.

IV. NON-COMPACT VORTEX CLUSTERS AND NON-PAIRWISE INTERACTIONS

Next we study the structure formation in a regime with relatively strong non-pairwise forces. In this section we consider a situation where the passive (i.e. with positive α_2) second band is coupled to the first band by extremely strong Josephson coupling $\eta = 7.0$ (shown on Fig. 12). This coupling imposes a strong energy penalty both for disparities of the condensates variations and for phase difference. The two and three body forces in that regime are shown in the middle column on Fig. 3. Indeed the two-body forces in this case have only a weak non-monotonicity. Importantly, there is an anisotropy of three body forces shown in Fig. 3. It clearly diminishes the energetic benefits of a triangle-like states compared to line-like vortex states. Identifying the ground states in this regime numerically (which involves four-body and higher order interactions) is much more complicated than in the previous cases. We get a flat and complicated energy landscape and the outcome of the energy minimization strongly depends on initial configuration (see Appendix for the description of numerical procedures). The Fig. 12 shows the typical non-universal outcome of the energy minimization in this case. Striking feature here is formation of vortex stripe-like configuration. Indeed it strongly contradicts the ground state structure predicted by the two-body forces in this system. Namely the axially symmetric two-body potentials with long range attraction and short-range repulsion (which we have in this case) do not allow stripe formation in the ground state configurations. Therefore the observation of the vortex stripes signals that the structure formation, along with short-range character of attractive tail, is influenced by repulsive multi-body forces in these cases (in contrast to the structure formation in the previous section which was dominated by two-body forces). Note that even in this regime, the system exhibits self-induced gradients of the phase difference, in spite of the strong Josephson coupling. In order to study the role of initial conditions we consider the vortex ordering in a similar regime but starting with 30 vortices placed at distances larger than the minimum of the two-body potential. If there were only two-body forces this vortex clusters would contract to minimize the energy. In contrast in the energy minimization process the vortex cluster first expands (see the animation of the evolution of the system in the numerical energy minimization process in the supplementary material¹⁵). Subsequently it breaks into a few sub-clusters and vortex chains. At the final stage of the evolution each cluster contracts. Final intervortex distances in each sub-cluster is smaller than intervortex distance in the initial state shown on Fig. 13.

Formation of highly disordered states and vortex chains due to short-range nature of the attractive potentials and many-body forces was a generic outcome of the simulation in the

similar type-1.5 regimes with strong Josephson coupling, in spite of negligible effects of ultra-fine numerical grid.

In this section we considered the regimes where the attractive part of two-body interaction was relatively weak and of short range. Physically, the fact that there are also multi-body forces which energetically penalize the hexagonal arrangement in large groups of vortices implies that at finite temperatures small clusters and irregular chain-like structures should easily form as well for entropic and kinetic reasons.

V. CONCLUSIONS.

In conclusion, in this work we investigated structures of vortex clusters in the Semi-Meissner state and demonstrated that *non-pairwise* interaction forces can be especially important in multicomponent and layered superconductors. It results in the very rich physics associated with the vortex clusters in type-1.5 regime. Namely N-quanta clusters can be quite different from simple superpositions of N single vortex solutions. In general they should have multiple local minima in the energy landscape. Thus vortex clusters can have extremely irregular shapes *even in absence of vortex pinning*. The discussed above regimes can be directly probed experimentally in type-I/type-II multilayers where intercomponent coupling can be tuned and be distinguished from pinning effects by *IV* characteristics. The found here non-pairwise forces should similarly be important in type-II multiband superconductors or layered structures for understanding compact configurations of pinned vortex clusters.

We also remark that in certain cases the separation into vortex and Meissner domains also implies phase separation into domains with different broken symmetries. Consider $U(1) \times U(1)$ model. Even if the second component there is not completely depleted in the vortex cluster, its density is suppressed and as a consequence the magnetic binding energy between vortices with different phase windings ($\Delta\theta_1 = 2\pi, \Delta\theta_2 = 0$) and ($\Delta\theta_1 = 0, \Delta\theta_2 = 2\pi$) can be arbitrarily small⁹. Moreover the vortex ordering energies in the component with more depleted density will also be small. As a result, even small thermal fluctuation can drive vortex sublattice melting transition¹⁰ in a macroscopically large vortex droplet. In that case the fractional vortices in weaker component tear themselves off the fractional vortices in strong component and form a disordered state. Note that the vortex sublattice melting is associated with the phase transition from $U(1) \times U(1)$ to $U(1)$ state¹⁰. I.e. that vortex cluster where one sublattice has melted will represent a domain of $U(1)$ phase (associated with the superconducting state of strong component) immersed in domain of vortexless $U(1) \times U(1)$ Meissner state.

We thank A. Gurevich and J.M. Speight for stimulating discussions. The work is supported by the NSF CAREER Award No. DMR-0955902, by Swedish Research Council, and by the Knut and Alice Wallenberg Foundation through the Royal Swedish Academy of Sciences fellowship. Computations were performed at the National Supercomputer Center (NSC) in Linköping, Sweden.

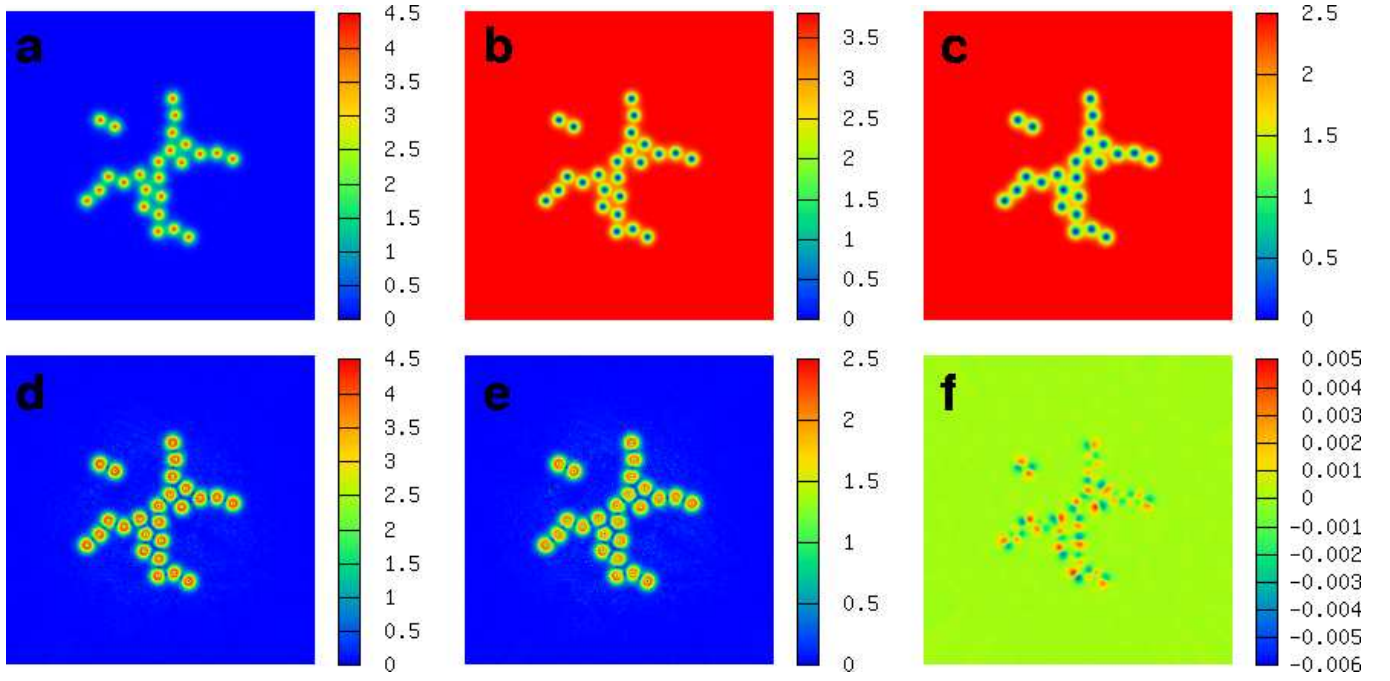


Figure 12. A bound state of an $N_v = 25$ vortex configuration in case when superconductivity in the second band is due to interband proximity effect and the Josephson coupling is very strong $\eta = 7.0$. The initial configuration in this simulation was a giant vortex. Other parameters are $(\alpha_1, \beta_1) = (-1.00, 1.00)$, $(\alpha_2, \beta_2) = (3.00, 0.50)$, $e = 1.30$.

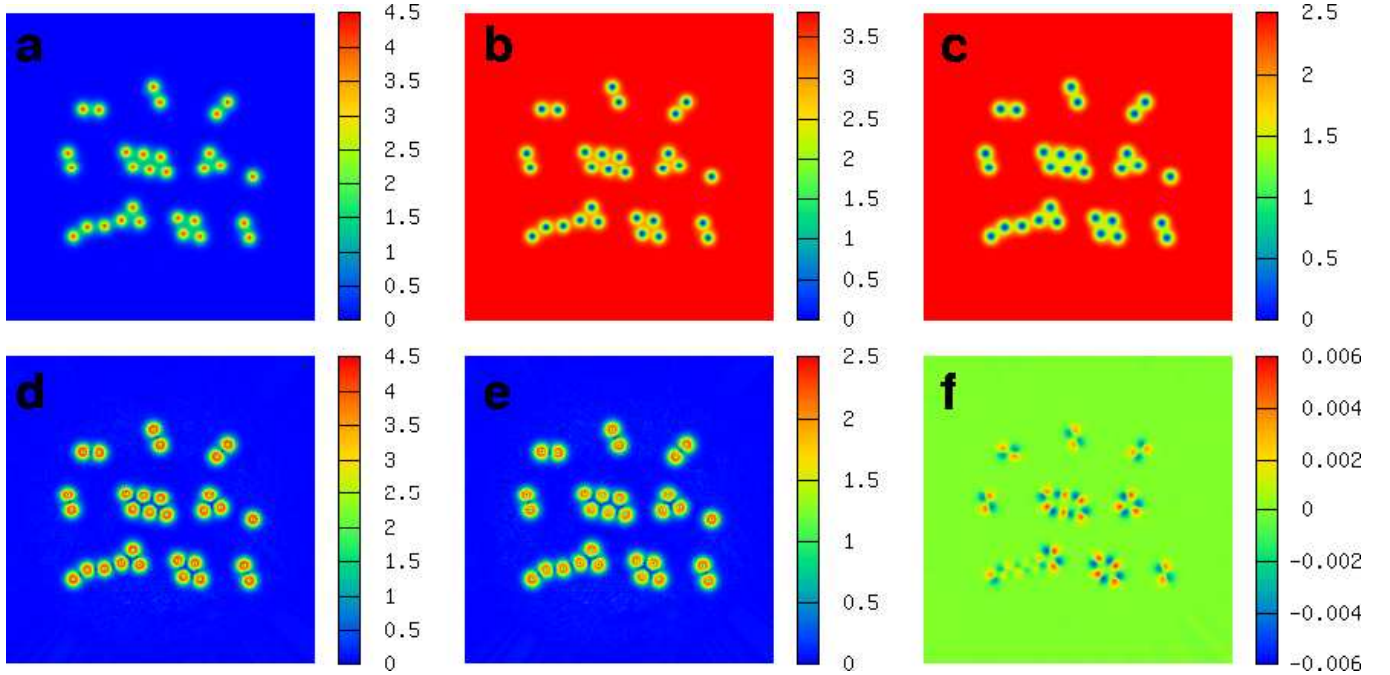


Figure 13. A bound state of an $N_v = 30$ vortex configuration for the system with parameters like in Fig. 12 which was obtained using a dilute initial configuration of vortices¹⁵.

Appendix A: Finite difference energy minimization

To calculate intervortex interaction energies we use finite difference energy minimization. Ground states of vortex sys-

tems and inter-vortex interaction energies are found by minimizing this functional subject to relevant constraints, such as vortex positions. To do this numerically, we discretize the system on a regular grid. To have the numerical results unbiased we use a non-adaptive grid where the grid spacing h is

the same everywhere in the domain. The Hamiltonian is then discretized using the finite difference approach:

Gradients are defined as

$$(\nabla f)_{i,i+1} = \frac{f(i+1) - f(i)}{h} \quad (\text{A1})$$

and magnetic flux is computed by line integration

$$B_{i,i+1,j,j+1} = \frac{1}{h^2} \oint_{\omega} \bar{A} \cdot d\bar{r} \quad (\text{A2})$$

where ω is the square with the corners $i, i+1, j, j+1$. The energy density in the grid point (i, j) then depends on function values in i, j and its neighbors.

The optimization scheme which is used in the first part of the paper is a modified version of the Newton-Raphson method. To minimize boundary effects we use free boundary conditions. Vortices are inserted using various initial configurations.

In order to calculate the inter-vortex interaction energy, we have to fix the position of vortices. Fixing a vortex position requires a special care to avoid the situation where the pinning substantially affects the vortex solution. We fix the vortex position by the following method. In the vortex center the condensate density is zero. We then fix the density only of the central point of the dominant component $|\psi_i|$ of the vortex to be zero in a given position of numerical grid. This effectively prevents the vortex from moving but does not prevent core splitting of $|\psi_1|$ and $|\psi_2|$ due to competing interactions. This “point pinning” method also has advantage of being a “minimally invasive” since only the position of the core singularity is fixed. Thus it allows calculate medium- and long-range forces with greatest accuracy.

However, at the same time, obviously, this method does not work for too short intervortex separation. For too short vortex separation it leads to the following easily identifiable artifact: a vortex core of one of the vortices elongates to be zero at both pinning centers allowing the second vortex to unpin and escape, while satisfying the energy minimization constraint. This behavior can be easily remedied by different pinning schemes. However for consistency and also because very short-distance intervortex forces are irrelevant for the questions studied in this paper we use one pinning procedure.

Convergence is determined as follows:

1) We choose a particular grid spacing h_1 and number of grid points $N_1 = N_{1x} \cdot N_{1y}$ giving a system size $L_x = h \cdot (N_{1x} - 1)$, $L_y = h \cdot (N_{1y} - 1)$. Then we minimize the energy until it does not change in a few thousand iterations. This gives us $E(h_1)$.

2) We decrease grid spacing h by a factor of 2 or 3 while retaining the system size L_x, L_y using spline interpolation. Then, we once again iterate until the energy does not change in a few thousand iterations, giving us $E(h_2)$ and so forth. We then determine convergence from

$$\frac{E(h_n) - E(h_{n+1})}{E(h_n)} = C. \quad (\text{A3})$$

We use grid sizes up to $N \approx 10^7$ which gives very high accuracy, typically $C < 10^{-4}$.

Appendix B: Finite element energy minimization

In the second part of the paper we use the unconstrained energy minimization. Bound state vortex configurations are minima of Ginzburg-Landau energy (1). This means that functional minimization of (1), from an appropriate initial state describing several flux quanta, should lead to bound state (if it exists). We consider the two-dimensional problem $\mathcal{F} = \int_{\Omega} F$ defined on the bounded domain $\Omega \subset \mathbb{R}^2$, supplemented by ‘open’ boundary conditions.

The variational problem is defined for numerical purpose using a finite element formulation provided by the Freefem++¹⁸ framework. Discretization within finite element formulation is done via a (homogeneous) triangulation on Ω , based on Delaunay-Voronoi algorithm. Functions are decomposed on a continuous piecewise quadratic basis on each triangle.

Contrary to the numerical method used in the first part, the accuracy does not depend only on the ‘number of grid points’. The accuracy of such method is controlled through the number of triangles, (we typically used 10^5), the order of expansion of the basis on each triangle (P2 elements are 2nd order polynomial basis on each triangle), and also the order of the quadrature formula for the integral on the triangles.

Once the problem is mathematically well posed, a numerical optimization algorithm is used to solve the variational non-linear problem (i.e. to find the minima of \mathcal{F}). We used here Nonlinear Conjugate Gradient method Algorithm is iterated until relative variation of the norm of the gradient of the functional \mathcal{F} with respect to all degrees of freedom is less than 10^{-6} . To be sure that our results are not numerical artifacts of this particular minimization scheme, we also performed standard Steepest Descent calculations and checked it leads to similar results.

Minimization starts with an initial guess: a field configuration carrying the N_v flux quanta described by

$$\Phi_a = u_a \prod_{i=1}^{N_v} \sqrt{\frac{1}{2} \left(1 + \tanh \left(\frac{4}{\xi_a} (\mathcal{R}_i(x, y) - \xi_a) \right) \right)} e^{i\Theta_i}, \quad \bar{A} = \frac{1}{e\mathcal{R}} (\sin \Theta, -\cos \Theta), \quad (\text{B1})$$

where $a = 1, 2$, u_a is the vacuum expectation value of each scalar field, the parameter ξ_a give the core sizes while Θ and

\mathcal{R} are

$$\begin{aligned}\Theta(x, y) &= \sum_{i=1}^{N_v} \Theta_i(x, y), \\ \Theta_i(x, y) &= \tan^{-1} \left(\frac{y - y_i}{x - x_i} \right), \\ \mathcal{R}(x, y) &= \sum_{i=1}^{N_v} \mathcal{R}_i(x, y), \\ \mathcal{R}_i(x, y) &= \sqrt{(x - x_i)^2 + (y - y_i)^2}.\end{aligned}\quad (\text{B2})$$

(x_i, y_i) are the initial position of a given vortex. Then, all degrees of freedom are relaxed simultaneously without *any* constraint to obtain high accurate solutions of the Ginzburg-Landau equations.

The initial guess (B1) allows starting from various very different initial configurations, depending on the values of the (x_i, y_i) . Since we know from two-body calculations, the preferred distance between two vortices, we choose to start either in the *repulsive* or in the *attractive* tail of the two-body interaction potential. Animations showing the evolution of the system from these various initial configurations, during the described above energy minimization is available as on-line supplementary material¹⁵. Note that we do not solve a dynamical problem here, the main purpose of these movies is that they reflect the structure of the free energy landscape and to give intuitive illustration of intervortex forces. For a reader interested in the a relationship between this energy minimization dynamics and the dynamics of Time Dependent Ginzburg-Landau model we refer to Ref.¹⁹.

The method described in the first part of the paper was also used for unconstrained simulations to doublecheck some of the results.

-
- ¹ N. S. Manton, P. Sutcliffe, *Topological solitons* Cambridge University Press, (2004).
² P. Gennes, *Superconductivity of metals and alloys*, Perseus Books, (1999).
³ E. Babaev, J. M. Speight, *Phys. Rev.* **B72**, 180502 (2005). E. Babaev, J. Carlström, M. Speight, *Phys. Rev. Lett.* **105**, 067003 (2010).
⁴ V. Moshchalkov, *et al.*, *Phys. Rev. Lett.* **102**, 117001 (2009), T. Nishio, *et al.*, *Phys. Rev. B* **81**, 020506 (2010).
⁵ J. Carlstrom, E. Babaev, M. Speight, *Phys. Rev. B* **83** 174509 (2011).
⁶ V. Dao, *et al.*, L. Chibotaru, T. Nishio, V. Moshchalkov, *Phys. Rev. B* **83**, 020503 (2011); R. Geurts, M. V. Milosevic, F. M. Peeters *Phys. Rev. B* **81**, 214514 (2010).
⁷ A. Gurevich, *Physica C* **456**, 160 (2007).
⁸ M. Silaev, E. Babaev, *Phys. Rev. B* **84**, 094515 (2011).
⁹ E. Babaev, *Phys. Rev. Lett.* **89**, 067001 (2002). E. Babaev, J. Jaykka, J.M Speight *Phys. Rev. Lett.* **103**, 237002 (2009).
¹⁰ E. Babaev, A. Sudbø, N. W. Ashcroft, *Nature* **431**, 666 (2004). J. Smiseth, E. Smorgrav, E. Babaev, and A. Sudbo *Phys.Rev.Lett.* **94** (2005) 096401
¹¹ E. Babaev, N. W. Ashcroft, *Nature Physics* **3**, 530 (2007)
¹² P. B. Jones, *Mon. Not. Roy. Astron. Soc.* **371**, 1327 (2006).
¹³ M. E. Peskin, *Ann. Phys. (N.Y.)* **113**, 122 (1978);
¹⁴ A.Chaves, F. M. Peeters, G. A. Farias, and M. V. Milosevic *Phys. Rev. B* **83**, 054516 (2011).
¹⁵ Movies can be found in the supplementary online material <http://link.aps.org/supplemental/.....> and at <http://people.umass.edu/garaud/NonPairwise.html>
¹⁶ E. Babaev, L. D. Faddeev, A. J. Niemi *Phys.Rev.B* **65**:100512, (2002) E. Babaev, *Phys. Rev.* **B79**, 104506 (2009).
¹⁷ R. Prozorov, A. F. Fidler, J. R. Hoberg, P. C. Canfield, *Nat Phys* **4**, 327 (2008).
¹⁸ F. Hecht, O. Pironneau, A. Le Hyaric, K. Ohtsuka, *Freefem++ (manual)* www.freefem.org (2007).
¹⁹ Q. Du, *Journal of Mathematical Physics*, AIP, **46** 095109 (2005)